Published in final edited form as:
Int J Biochem Cell Biol. 2009 December ; 41(12): 2578–2587. doi:10.1016/j.biocel.2009.08.015.

Drug transporter, P-glycoprotein (MDR1), is an integrated component of the mammalian blood-testis barrier[§]

Linlin Su, C., **Yan Cheng**, and **Dolores D. Mruk**
Population Council, Center for Biomedical Research, 1230 York Avenue, New York 10065

Abstract

Throughout spermatogenesis, leptotene spermatocytes traverse the blood-testis barrier (BTB) to enter the adluminal compartment of the seminiferous epithelium for continued development. At the same time, the integrity of the BTB, which is constituted by co-existing tight junctions (TJ), basal ectoplasmic specializations (basal ES) and desmosome-like junctions, must be maintained since a breach in barrier function can result in spermatogenic arrest and infertility. There is evidence to suggest that drug transporters may function at the BTB, but little is known about how they contribute to spermatogenesis. In this study, we investigate the role of P-glycoprotein (P-gp), a drug efflux pump, in BTB dynamics. A survey by RT-PCR revealed several transport proteins to be expressed by the testis, including *Mdr1* (gene symbol for P-gp), *Mrp1*, *Abcc5* and *Slc15a1*. It was also demonstrated that P-gp localizes to the BTB in all stages of the epithelial cycle in the adult rat testis, as well as to the Sertoli cell elongated spermatid interface in stages VII–VIII. We continued our study by examining the levels of several transporters in the testis following oral administration of Adjudin, a compound known to affect Sertoli-germ cell adhesion. In this experiment, the steady-state levels of P-gp, MRP1, ABCG1 and SLC15A1 were all found to increase by several-fold within hours of Adjudin treatment during junction restructuring. More importantly, an increase in P-gp association with TJ proteins (*e.g.*, occludin, claudin-11 and JAM-A) was noted when testis lysates from Adjudin-treated rats were used for co-immunoprecipitation experiments, suggesting that P-gp may enhance BTB function during Sertoli-germ cell junction restructuring.

Keywords

testis; blood-testis barrier; Sertoli cell; tight junction; P-glycoprotein

Introduction

Spermatogenesis is a complex process that requires the integrity of the blood-testis barrier (BTB) to be maintained since a compromise in BTB function can result in exposure of unique haploid germ cell antigens to the host's immune system and infertility (Hedger and Hales, 2006). Several different types of junctions are known to contribute to BTB integrity, including tight junctions (TJ), basal ectoplasmic specializations (basal ES) and desmosome-like junctions, and except for the last type of junction, we have a relatively good understanding of their molecular architecture and regulation in the testis (Mruk and Cheng, 2004b, Mruk and

Address all correspondence to: Dolores D. Mruk, Ph.D., Population Council, Center for Biomedical Research, 1230 York Avenue, New York, NY 10065, Phone: (212) 327 8738, Fax: (212) 327 8733, mruk@popcbr.rockefeller.edu.

Cheng, 2004a, Mruk et al., 2008). In this study, we aim to expand our knowledge of BTB dynamics by looking beyond conventional TJ and basal ES proteins present at the BTB. Instead, we were interested in determining whether drug transporters, such as P-glycoprotein (P-gp), function at the BTB possibly to maintain the integrity of the seminiferous epithelium.

P-gp [product of *Abcb1* gene, also known as multidrug resistance 1 (*Mdr1*) gene] is the best-studied ATP-binding cassette (ABC) transporter of the MDR/transporter associated with antigen processing (TAP) subfamily and the focus of this study. First described as a protein that was over-expressed in tumor cells displaying resistance to anticancer drugs, P-gp was subsequently reported to be an ATP-powered efflux pump whose role is to protect organisms from toxic substances by transporting compounds out of cells against steep concentration gradients (Loscher and Potschka, 2005, Mizuno et al., 2003, Leslie et al., 2005, Miller et al., 2008). P-gp substrates generally include lipophilic and amphiphatic compounds ranging from ~300–4000 Da. P-gp is also known to transport Ca^{2+} channel blockers, HIV protease inhibitors, immunosuppressants, antibiotics, statins and steroids. In addition, P-gp expression is wide-spread and not restricted to tumor cells; expression has also been reported in organs with excretory roles (*e.g.*, liver, kidney and small intestine) and at blood-tissue barriers (*e.g.*, blood-brain, blood-testis and blood-placenta) where it functions to restrict entry of a drug or to facilitate the rapid elimination of a drug from sensitive tissues (Fojo et al., 1987, Thiebaut et al., 1987). Indeed, a study using transgenic knockout mice illustrated that P-gp is critical for blood-tissue barrier function because animals had a disrupted blood-brain barrier, as well as sensitivity to ivermectin (a broad-spectrum anti-parasitic drug) and vinblastine [an anti-mitotic drug used to treat certain types of cancers] (Schinkel et al., 1994). While these animals were viable and fertile, knockdown of *Mdr1* affected drug pharmacokinetics and elimination, and in the case of ivermectin, even resulted in death. In another study, inhibition of P-gp by LY-335979 (presently undergoing Phase III Clinical Trials for the treatment of leukemia and myelodysplastic syndromes) increased the concentration of nelfinavir, an HIV protease inhibitor, in the brain and testis by several-fold (Choo et al., 2000), revealing that P-gp has a protective role at blood-tissue barriers.

In this study, we report that P-gp is an integrated component of the BTB in the adult rat. Equally important, when the seminiferous epithelium was under assault by Adjudin [a compound that is known to specifically affect Sertoli-germ cell adhesion (Cheng et al., 2001, Grima et al., 2001, Mruk et al., 2006, Cheng et al., 2005)], P-gp associated more with TJ proteins, suggesting that P-gp may enhance BTB function during Sertoli-germ cell restructuring. The results of this study illustrate P-gp's participation in cell junction dynamics.

Materials and Methods

Animals

Male Sprague Dawley rats at 20 and 90 days of age were purchased (Charles River Laboratories, Kingston, NY) and allowed to acclimatize for 24–48 hr before experimental use. Rats had free access to water and standard rat chow, and they were exposed to 12 hr light:dark cycles. Rats were sacrificed by CO_2 asphyxiation as directed (Beaver et al., 2001). The use of animals was approved by The Rockefeller University Animal Care and Use Committee with protocol numbers 06018 and 09016.

Isolation of Sertoli cells

Sertoli cells were isolated from 20-day old rats and plated on Matrigel™- coated coverslips at 0.05×10^6 cells/cm^2 in F12/DMEM supplemented with growth factors as described (Mruk et al., 2003, Cheng et al., 1986). Contaminating germ cells were removed 48 hr after plating by treatment with a hypotonic buffer (Galdieri et al., 1981) to yield Sertoli cells with a purity of

~98%. Cells were incubated at 35 °C in a humidified atmosphere of 5% CO_2/95% air [v/v] for an additional 48 hr. These cells were then used for immunofluorescent microscopy experiments.

Treatment of animals with Adjudin

A single dose of Adjudin (50 mg/kg b.w., suspended in 0.5% methyl-cellulose [w/v]) was orally administered to adult rats (~300 gm b.w., n = 7/time point) to induce germ cell loss from the seminiferous epithelium (Cheng et al., 2001, Grima et al., 2001). Rats were killed at different time points ranging from a few hours to several days after treatment. Testes were removed, frozen in liquid nitrogen and stored at −80 °C until used for lysate preparation or for immunofluorescent microscopy. Control rats (n = 7) received 0.5% methyl-cellulose [w/v] only.

RT-PCR

Total RNA was extracted from the testis, kidney, liver and brain of adult male rats by RNA STAT-60 (Tel-test “B” Inc., Friendswood, TX). Two μg RNA was then used for the reverse transcriptase reaction, followed by PCR as described (Mruk et al., 1997, Mruk et al., 1998) (Table 1). Contamination of samples by genomic DNA was assessed by omitting reverse transcriptase during cDNA synthesis. Primers were designed to anneal specifically to transcripts as deposited in GenBank® (Table 1), and *S-16* was used as an internal control to ensure equal sample processing. After electrophoresis, gels were stained with ethidium bromide, and images were captured with a Syngene Bio Imaging system (Cambridge, England). Nucleotide sequencing was performed to verify the authenticity of transcripts detected in the testis.

Immunoblotting

Tissue lysates were prepared in lysis buffer (10 mM Tris, pH 7.4 at 22 °C containing 0.15 M NaCl, 10% glycerol [v/v], 1% NP-40 [v/v], protease and phosphatase inhibitors) by using a tissue:buffer ratio of 1:5. Approximately 75–100 μg lysate was resolved onto SDS polyacrylamide gels (SDS-PAGE) under reducing conditions as described (Lau and Mruk, 2003). Gels were transferred onto nitrocellulose, blocked with 5% milk [w/v] in PBS-Tris, pH 7.4 containing 0.1% Tween-20 [v/v] for 1 hr and probed with different antibodies at R.T. overnight (Table 2). The following day, blots were incubated with HRP-conjugated secondary antibodies (1:1000, Santa Cruz Biotechnology, Santa Cruz, CA), and chemiluminescence was used to detect immunoreactive proteins. Images were captured with a LAS-4000 luminescent image analyzer (FujiFilm, Valhalla, NY).

Enzyme immunohistochemistry

To localize P-gp in the adult rat testis, enzyme immunohistochemistry was performed using the HistoMouse™-MAX kit (Zymed/Invitrogen) which was compatible with mouse, rabbit and guinea pig primary antibodies. In brief, animals were killed, testes removed and frozen immediately in liquid nitrogen. Thereafter, testes were embedded in Tissue-Tek Optimal Cutting Temperature (O.C.T) compound (Sakura Finetek USA, Inc., Torrance, CA), 7 μm-thick sections obtained, mounted onto poly-L-lysine-coated glass slides and dried briefly. Sections were then saturated with Bouin’s fixative, washed with PBS, pH 7.4 and endogenous peroxidase activity quenched with 3% H_2O_2 [v/v] in methanol. Sections were blocked with 10% normal goat serum (NGS, [v/v]) for 1 hr and incubated with P-gp IgG (1:50; stock concentration, 200 μg/ml, Table 2) in PBS containing 1% NGS [v/v] at R.T. overnight. The next day, sections were saturated with a broad spectrum horseradish peroxidase (HRP)-conjugated secondary antibody, followed by color development with 3-amino-9-ethylcarbazole (AEC). Nuclei were visualized by hematoxylin. Mouse IgG (1:50; stock

concentration, 200 μg/ml) was used as the control. Images were acquired with MicroSuite FIVE software (Version 1.224, Olympus Soft Imaging Solutions Corp, Lakewood, CO) and an Olympus DP70 12.5 MPa digital camera attached to an Olympus BX61 motorized microscope. Images were adjusted for brightness and contrast only with Adobe Photoshop software (Version 10.0).

Immunofluorescent microscopy

Immunofluorescent microscopy was performed using adult rat testes and primary Sertoli cells (0.05×10^6 cells/cm^2, day 4 after plating). Sertoli cells were fixed in 4% paraformaldehyde [w/v], permeabilized with 0.1% Triton X-100 [v/v] and blocked with 10% NGS [v/v]. Thereafter, cells were incubated with a mixture of antibodies from two different species (*e.g.*, P-gp IgG + occludin IgG) in PBS containing 1% NGS [v/v] at R.T. overnight (Table 2). Cells were then washed and incubated with Alexa Fluor 488 and 555 (1:100) secondary antibodies in PBS containing 10% NGS [v/v]. ProLong Gold antifade reagent with DAPI was used for mounting, and images were acquired as described above. Immunofluorescent microscopy using adult rat testes was performed by a similar protocol (Sarkar et al., 2008,Sarkar et al., 2006).

Co-immunoprecipitation

Approximately 500 μg lysate from control or Adjudin-treated rat testes was used for co-immunoprecipitation (Co-IP) as described (Lau and Mruk, 2003, Sarkar et al., 2006). Lysates were first pre-cleared with rabbit IgG, and interacting proteins were precipitated with protein A/G PLUS agarose (Santa Cruz Biotechnology). Thereafter, supernatants were incubated with either occludin, claudin-11, junctional adhesion molecule-A (JAM-A) or rabbit IgG (~2–5 μg, Table 2) overnight, and protein A/G PLUS agarose was used to pull-down interacting proteins. Agarose beads were washed 4 times with gentle rotation for a total of 1.5 hr with lysis buffer containing protease and phosphatase inhibitors. SDS sample buffer (0.125 M Tris, pH 6.8 at 22 °C containing 20% glycerol [v/v], 1% SDS [w/v] and 1.6% 2-mercaptoethanol [v/v]) was then added to agarose beads, and this was heated at 60 °C as instructed on the P-gp antibody specification sheet provided by the vendor. After centrifugation, samples were subjected to SDS-PAGE, followed by immunoblotting with a P-gp antibody (Table 2).

General methods

Protein estimation was performed by using the Bio-Rad D_C Protein Assay (Bio-Rad, Hercules, CA). Scion Image (Version 1.1, NIH, Bethesda, MD) and GB-STAT (Version 7.0, Dynamic Microsystems, Silver Spring, MD) software packages were used to digitize gel images and determine statistical significance, respectively. In some cases, the UN-SCAN-IT gel software package (Version 6.1, Silk Scientific, Orem, Utah) was used to verify the accuracy of scanning results obtained by Scion Image. Within UN-SCAN-IT gel software, background correction and saturation checking were applied to gel images, and saturated images were not densitometrically scanned. Multiple comparisons were done by ANOVA with Dunnett's test. $P<0.05$ was taken as statistically significant. All RT-PCR, immunoblotting and co-immunoprecipitation experiments were repeated 4–7 times; all enzyme immunohistochemistry and immunofluorescent experiments were repeated 3 times each using different testes or batches of isolated Sertoli cells.

Results

Efflux and influx pumps are expressed by the testis

There are few reports investigating the role of drug transporters in the testis (Melaine et al., 2002, Melaine et al., 2006, Morales et al., 2008, Dalton et al., 2005, Ono et al., 2007), and most

studies have focused on understanding how drug resistance can be overcome in cancer cells *in vitro* and *in vivo* (Loscher and Potschka, 2005, Mizuno et al., 2003, Doyle and Ross, 2003, Robey et al., 2009). One of the aims of this study was to determine whether efflux and influx pumps are expressed by the testis. In this initial experiment, we did not restrict our survey to drug/xenobiotic transporters; we also included transport proteins that are known to transport a wide variety of substrates such as lipids, steroids and ions (Leslie et al., 2005, Borst et al., 2000, van Meer et al., 2006, Seeger and van Veen, 2008, Kusuhara and Sugiyama, 2007, Meredith, 2009). By RT-PCR (Table 1), we report that several transporters are expressed by the testis, including efflux pumps: *Mdr1*, *Mrp1*, *Abcb8*, *Abcc5*, *Abce1*, *Atp7a*, *Slc16a1* and *Slc33a1* (Figure 1A), and influx pumps: *Slc15a1*, *Slc22a3*, *Slc22a15*, *Slco4a1*, *Slco6b1* and *Slco6c1* (Figure 1B). Many of these genes are also expressed by the kidney, liver and brain. Of the transport proteins investigated here, *Slco6c1* expression was restricted to the testis (Figure 1B), consistent with a previous report (Suzuki et al., 2003). Immunoblotting confirmed the presence of P-gp, MRP1 and SLC15A1 in these organs (Figure 1A, B; Table 2). We did not include immunoblots for all of the other genes presented in this figure because in most cases antibodies were not commercially available.

P-gp localizes to the BTB and elongated spermatids in the seminiferous epithelium

Enzyme immunohistochemistry revealed that P-gp localizes to the site of the BTB at all stages of the seminiferous epithelial cycle in adult rats, as well as to the lumenal edge surrounding elongated spermatids at stages VII–VIII at the site of the apical ectoplasmic specialization [apical ES] (Figure 2A). A significantly weaker signal was also observed with round and elongating spermatids. Outside of the seminiferous epithelium, strong P-gp immunoreactivity was detected in the tunica propria (*i.e.*, peritubular myoid cells), interstitium (*i.e.*, Leydig cells) and blood vessel endothelium. Incubating sections with mouse IgG at the same dilution that was used for P-gp IgG yielded no observable staining (Figure 2A). P-gp antibody monospecificity was assessed by immunoblotting, and a single 170 kDa protein band was observed in Sertoli cell and testis lysates (Figure 2B), illustrating that this antibody is suitable for enzyme immunohistochemistry and immunofluorescent microscopy experiments (Table 2).

P-gp co-localizes with TJ and basal ES proteins

Figure 2A showed that P-gp was present at the site of the BTB in adult rats. To further expand this observation, we performed immunofluorescent microscopy to assess whether P-gp co-localizes with BTB constituent proteins. Consistent with enzyme immunohistochemistry results (Figure 2A), P-gp staining was noted at the BTB (Figure 3A). When corresponding images were merged, P-gp was found to co-localize with occludin, claudin-11, JAM-A, zonula occludens-1 (ZO-1), N-cadherin and β-catenin (Figure 3A). By immunofluorescent microscopy, P-gp staining was also observed at the site of elongated spermatids, as well as in the tunica propria (*i.e.*, peritubular myoid cells) and endothelium of blood vessels (Figure 3A). When primary Sertoli cells were cultured for 4 days in order to establish a Sertoli cell barrier and used for immunofluorescent microscopy, P-gp co-localized with occludin, JAM-A, ZO-1, N-cadherin and β-catenin at the Sertoli-Sertoli cell surface (Figure 3B). We were also able to detect P-gp within the cytoplasm, albeit the immunoreactive signal was weaker.

Up-regulation of steady-state levels of efflux/influx pumps and changes in protein-protein interactions following administration of Adjudin

The steady-state level of different efflux and influx pumps following administration of Adjudin was investigated in the testis by immunoblotting. The density of both P-gp and MRP1 was shown to increase by several-fold (Figure 4A), coinciding with the time that [^{3}H]-Adjudin peaked in the testis at 3–16 hr (Cheng et al., 2005). ABCG1 and SLC15A1 were also induced

significantly after Adjudin treatment, but these changes were delayed when compared to P-gp and MRP1 (Figure 4A). Before investigating whether there were any changes in protein-protein interactions, the steady-state levels of occludin, claudin-11 and JAM-A were examined by immunoblotting. Except for occludin which was up-regulated on day 1 after Adjudin treatment, no changes were observed for claudin-11 and JAM-A (Figure 4B). When testis lysates from control and Adjudin-treated rats were used for co-immunoprecipitation, P-gp was shown to associate more with occludin, claudin-11 and JAM-A from ~6 hr-1 day post-treatment (Figure 4C). Substituting occludin, claudin 11 and JAM-A IgG with rabbit IgG (negative control) in co-immunoprecipitation reactions did not pull-down interacting proteins (Figure 4C). To verify results shown in Figure 4A–C, we co-localized P-gp with occludin in control and Adjudin-treated rat testes by immunofluorescent microscopy (Figure 4D). Following treatment at 9 hr, there was an increase in P-gp at the site of the BTB, as well as with peritubular myoid cells and blood vessel endothelia. By day 1, the intensity of the P-gp immunofluorescent signal was indistinguishable from the control. Changes in occludin localization were not noted at 9 hr and 1 day post-treatment. When corresponding images were merged, co-localization of P-gp with occludin was evident after Adjudin treatment (Figure 4D).

Discussion

P-gp is an integrated component of the BTB

The primary aim of this study was to determine whether P-gp has a role in BTB dynamics. A survey by RT-PCR revealed that several efflux and influx transport pumps are expressed by the testis, including *Mdr1*, *Mrp1*, *Slc15a1* and *Slco6c1*. Of the several transport pumps investigated in this study, MDR1 (*i.e.,* P-gp) has been studied the most extensively in the context of overcoming chemo- resistance. Interestingly, P-gp was also postulated to function as a ‘gatekeeper’ at different blood-tissue barriers (Fromm, 2004), but its precise role within these structures has not yet been defined. Indeed, an enzyme immunohistochemistry experiment illustrated that P-gp localized to the site of the BTB in a ring-like pattern in all stages of the seminiferous epithelial cycle. However, this is in contrast to a previously published study by Melaine and colleagues which failed to detect P-gp at the BTB in testes from several species, including the rat (Melaine et al., 2002). This inconsistency in data between Melanie’s and our study is likely to be due to differences in the antibodies used and/or tissue processing (*i.e.,* Melanie *et al.,* used paraffin-embedded sections). This immunohistochemistry experiment was further expanded by immunofluorescent microscopy to show that P-gp co-localized with several BTB component proteins (*e.g.,* occludin, claudin-11, JAM-A, ZO-1, N-cadherin and β-catenin). Similar results were obtained when primary Sertoli cells having an established Sertoli cell barrier were used for immunofluorescent microscopy; P-gp co-localized with TJ and basal ES proteins at the Sertoli-Sertoli cell surface. In Sertoli cells, we were also able to detect P-gp within the cytoplasm. Although localization at the plasma membrane is required for P-gp to function as an efflux pump, P-gp can also transit between the plasma membrane and endosomes in MCF-7 (human breast carcinoma) and S1-B1 (human intestinal carcinoma) cells (Kim et al., 1997, Fu and Roufogalis, 2007), suggesting that P-gp may have additional functions. Taken collectively, these results reveal that P-gp is an integrated component of the BTB.

What is the possible role of P-gp at the BTB?

Following administration of Adjudin to adult rats, the steady-state levels of P-gp, MRP1, ABCG1 and SLC15A1 increased several hours after treatment. Generally speaking, up-regulation of transport proteins such as P-gp in other organs is known to result in drug efflux and to contribute to therapeutic resistance which is often seen in individuals diagnosed with cancer or HIV/AIDS (Mizuno et al., 2003). Interestingly, the steady-state levels of P-gp and MRP1 increased several hours after Adjudin was administered orally, coinciding with the time

that [^{3}H]-Adjudin peaked in the testis at 3–16 hr (Cheng et al., 2005). By the time [^{3}H]-Adjudin was cleared from the testis at ~24 hr (Cheng et al., 2005), both P-gp and MRP1 had returned to their basal levels, suggesting that these two transport pumps may be functioning in the elimination of Adjudin from the testis. It is also worth noting that P-gp localized to peritubular myoid cells and that an increase in myoid cell-associated P-gp immunoreactivity was observed following Adjudin administration. This is interesting because in rodents peritubular myoid cells are known to contribute, at least to some extent, to BTB function (Fawcett et al., 1970, Dym and Fawcett, 1970). As such, it is possible that myoid cells also function in the protection of the seminiferous epithelium from unwanted agents and drugs.

When testis lysates from control and Adjudin-treated rats were used for co-immunoprecipitation, P-gp increased its association with occludin, claudin-11 and JAM-A. Except for P-gp and occludin, which were both up-regulated after Adjudin treatment, changes in protein-protein interactions (*i.e.*, P-gp/claudin-11 and P-gp/JAM-A) are not likely to be the result of inherent increases in steady-state protein levels. Given its role in the elimination of drugs/xenobiotics from tissues, why would P-gp interact with more occludin, claudin-11 and JAM-A in the testis following Adjudin treatment? We hypothesize that P-gp interacts with these proteins to enhance BTB function (Figure 5), in turn blocking further entry of Adjudin into the seminiferous epithelium which may otherwise result in permanent infertility. In a separate but closely-related study, we have taken it upon ourselves to investigate TJ function in Adjudin-treated Sertoli cells, a different system from the *in vivo* one used in this study because no germ cells are present. To our surprise, the steady-state levels of several TJ proteins (*e.g.*, claudin-11, ZO-1 and CAR) surged dose-dependently following Adjudin treatment. This coincided with an increase in the tightness of the Sertoli cell barrier when its function was assessed by transepithelial electrical resistance measurements (Su, Cheng and Mruk, unpublished observations). These findings seemingly suggest that a unique mechanism is in place to protect BTB integrity during extensive restructuring of Sertoli-germ cell junctions.

The emerging role of P-gp in junction dynamics is supported by a few other studies in the literature. For example, P-gp was shown to co-localize and co-immunoprecipitate with actin, as well as with ezrin, radixin and moesin (ERM) (Luciani et al., 2002), a small family of adaptor proteins involved in linking transmembrane proteins to actin filaments (Bretscher, 1999). When antisense oligonucleotides were used to inhibit ERM function, P-gp–actin interactions were lost and P-gp-mediated drug transport was adversely affected (Luciani et al., 2002), illustrating that P-gp–actin and P-gp–ERM binding are critical for drug efflux. Furthermore, actin-perturbing compounds have been shown to directly affect P-gp function. Cytochalasin D down-regulated P-gp expression in hepatocytes (Lee et al., 1995) and enhanced drug accumulation in another cell type, leukemia cells (Tsuruno and Iida, 1986). At this point, we question whether P-gp is absolutely essential for barrier function. We are particularly interested in determining whether specific knockdown of P-gp by RNAi in Sertoli cells can transiently ‘open’ the permeability barrier and whether this can affect Adjudin entry. We anticipate that future studies will provide new and important insights on the dual role of P-gp in therapeutic resistance and cell junction dynamics.

Acknowledgments

This work was supported in part by NICHD, NIH (1R03HD061401-01 to DDM, and R01HD056034, R03 HD051512 and U54HD029990 Project 5 to CYC). LS is the recipient of a Graduate Student Fellowship from Hong Kong University, Hong Kong.

Abbreviations

ABC ATP-binding cassette

basal ES	basal ectoplasmic specialization
BTB	blood-testis barrier
Co-IP	co-immunoprecipitation
ERM	ezrin, radixin and moesin
HRP	horseradish peroxidase
JAM-A	junctional adhesion molecule-A
MDR1	multidrug resistance 1
MRP1	multiple drug resistance protein 1
NGS	normal goat serum
P-gp	P-glycoprotein
RT-PCR	reverse transcription-polymerase chain reaction
SLC	solute carrier
TJ	tight junction
ZO-1	zonula occludens-1

References

Beaver BV, Reed W, Leary S, McKiernan B, Bain F, Schultz R, Bennett BT, Pascoe P, Shull E, Cork LC, Francis-Floyd R, Amass KD, Johnson R, Schmidt RH, Underwood W, Thorton GW, Kohn B. 2000 Report of the American Veterinary Medical Association Panel in Euthanasia. J Am Vet Med Assoc 2001;218:669–96. [PubMed: 11280396]

Borst P, Zelcer N, van Helvoort A. ABC transporters in lipid transport. Biochim Biophys Acta 2000;1486:128–44. [PubMed: 10856718]

Bretscher A. Regulation of cortical structure by the ezrin-radixin-moesin protein family. Curr Opin Cell Biol 1999;11:109–16. [PubMed: 10047517]

Cheng CY, Mather JP, Byer AL, Bardin CW. Identification of hormonally responsive proteins in primary Sertoli cell culture medium by anion-exchange high performance liquid chromatography. Endocrinology 1986;118:480–8. [PubMed: 3080306]

Cheng CY, Mruk D, Silvestrini B, Bonanomi M, Wong CH, Siu MKY, Lee NPY, Lui WY, Mo MY. AF-2364 [1-(2,4-dichlorobenzyl)-1*H*-indazole-3-carbohydrazide] is a potential male contraceptive: a review of recent data. Contraception 2005;72:251–61. [PubMed: 16181968]

Cheng CY, Silvestrini B, Grima J, Mo MY, Zhu LJ, Johansson E, Saso L, Leone MG, Palmery M, Mruk D. Two new male contraceptives exert their effects by depleting germ cells prematurely from the testis. Biol Reprod 2001;65:449–61. [PubMed: 11466213]

Choo EF, Leake B, Wandel C, Imamura H, Wood AJ, Wilkinson GR, Kim RB. Pharmacological inhibition of P-glycoprotein transport enhances the distribution of HIV-1 protease inhibitors into brain and testis. Drug Metab Dispos 2000;28:655–60. [PubMed: 10820137]

Dalton TP, He L, Wang B, Miller ML, Jin L, Stringer KF, Chang X, Baxter CS, Nebert DW. Identification of mouse SLC39A8 as the transporter responsible for cadmium-induced toxicity in the testis. Proc Natl Acad Sci USA 2005;102:3401–6. [PubMed: 15722412]

Doyle LA, Ross DD. Multidrug resistance mediated by the breast cancer resistance protein BCRP (ABCG2). Oncogene 2003;22:7340–58. [PubMed: 14576842]

Dym M, Fawcett DW. The blood-testis barrier in the rat and the physiological compartmentation of the seminiferous epithelium. Biol Reprod 1970;3:308–26. [PubMed: 4108372]

Fawcett DW, Leak LV, Heidger PM. Electron microscopic observations on the structural components of the blood-testis barrier. J Reprod Fertil 1970;10(Suppl 10):105–22.

Fojo AT, Ueda K, Slamon DJ, Poplack DG, Gottesman MM, Pastan I. Expression of a multidrug-resistance gene in human tumors and tissues. Proc Natl Acad Sci USA 1987;84:265–9. [PubMed: 2432605]

Fromm MF. Importance of P-glycoprotein at blood-tissue barriers. Trends Biochem Sci 2004;25:423–9.

Fu D, Roufogalis BD. Actin disruption inhibits endosomal traffic of P-glycoprotein-EGFP and resistance to daunorubicin accumulation. Am J Physiol Cell Physiol 2007;292:C1543–52. [PubMed: 17122416]

Galdieri M, Ziparo E, Palombi F, Russo MA, Stefanini M. Pure Sertoli cell cultures: a new model for the study of somatic-germ cell interactions. J Androl 1981;5:249–59.

Grima J, Silvestrini B, Cheng CY. Reversible inhibition of spermatogenesis in rats using a new male contraceptive, 1-(2,4-dichlorobenzyl)-indazole-3-carbohydrazide. Biol Reprod 2001;64:1500–8. [PubMed: 11319158]

Hedger, MP.; Hales, DB. Immunophysiology of the male reproductive tract. In: Neill, JD., editor. Knobil and Neill's Physiology of Reproduction. New York: Elsevier; 2006. p. 1195-286.

Kim HC, Barroso M, Samanta R, Greenberger L, Sztul E. Experimentally induced changes in the endocytic traffic of P-glycoprotein alter drug resistance of cancer cells. Am J Physiol 1997;273:C687–702. [PubMed: 9277367]

Kusuhara H, Sugiyama Y. ATP-binding cassette, subfamily G (ABCG family). Pflugers Arch-Eur J Physiol 2007;453:735–44. [PubMed: 16983557]

Lau ASN, Mruk DD. Rab8B GTPase and junction dynamics in the testis. Endocrinology 2003;144:1549–63. [PubMed: 12639940]

Lee CH, Bradley G, Ling V. Overexpression of the class II P-glycoprotein gene in primary rat hepatocyte culture: evidence for increased mRNA stability. Cell Growth Differ 1995;6:347–54. [PubMed: 7794802]

Leslie EM, Deeley RG, Cole SPC. Multidrug resistance proteins: role of P-glycoprotein, MRP1, MRP2, and BCRP (ABCG2) in tissue defense. Toxicol Appl Pharmacol 2005;204:216–37. [PubMed: 15845415]

Loscher W, Potschka H. Drug resistance in brain diseases and the role of drug efflux transporters. Nat Rev Neurosci 2005;6:591–602. [PubMed: 16025095]

Luciani F, Molinari A, Lozupone F, Calcabrini A, Lugini L, Stringaro A, Puddu P, Arancia G, Cianfriglia M, Fais S. P-glycoprotein-actin association through ERM family proteins: a role in P-glycoprotein function in human cells of lymphoid origin. Blood 2002;99:641–8. [PubMed: 11781249]

Melaine N, Lienard MO, Dorval I, Le Goascogne C, Lejeune H, Jegou B. Multidrug resistance genes and P-glycoprotein in the testis of the rat, mouse, guinea pig, and human. Biol Reprod 2002;67:1699–707. [PubMed: 12444043]

Melaine N, Satie AP, Lassurquere J, Desmots S, Jegou B, Samson M. Molecular cloning of several rat ABC transporters including a new ABC transporter, Abcb8, and their expression in rat testis. Int J Androl 2006;29:392–9. [PubMed: 16390497]

Meredith D. The mammalian proton-coupled peptide cotransporter PepT1: sitting on the transporter-channel fence? Phil Trans R Soc B 2009;364:203–7. [PubMed: 18957377]

Miller DS, Bauer B, Hartz AMS. Modulation of P-glycoprotein at the blood-brain barrier: opportunities to improve central nervous system pharmacotherapy. Pharmacol Rev 2008;60:196–209. [PubMed: 18560012]

Mizuno N, Niwa T, Yotsumoto Y, Sugiyama Y. Impact of drug transporter studies on drug discovery and development. Pharmacol Rev 2003;55:425–61. [PubMed: 12869659]

Morales CR, Marat AL, Ni X, Yu Y, Oko R, Smith BT, Argraves WS. ATP-binding cassette transporters ABCA1, ABCA7 and ABCG1 in mouse spermatozoa. Biochem Biophys Res Commun 2008;376:472–7. [PubMed: 18793613]

Mruk D, Cheng CH, Cheng YH, Mo MY, Grima J, Silvestrini B, Lee WM, Cheng CY. Rat testicular extracellular superoxide dismutase (SOD_{EX}): its purification, cellular distribution, and regulation. Biol Reprod 1998;59:298–308. [PubMed: 9687299]

Mruk D, Zhu LJ, Silvestrini B, Lee WM, Cheng CY. Interactions of proteases and protease inhibitors in Sertoli-germ cell cocultures preceding the formation of specialized Sertoli-germ cell junctions *in vitro*. J Androl 1997;18:612–22. [PubMed: 9432134]

Mruk DD, Cheng CY. Cell-cell interactions at the ectoplasmic specialization in the testis. Trends Endocrinol Metab 2004a;15:439–47. [PubMed: 15519891]

Mruk DD, Cheng CY. Sertoli-Sertoli and Sertoli-germ cell interactions and their significance in germ cell movement in the seminiferous epithelium during spermatogenesis. Endocr Rev 2004b;25:747–806. [PubMed: 15466940]

Mruk DD, Silvestrini B, Cheng CY. Anchoring junctions as drug targets: role in contraceptive development. Pharmacol Rev 2008;60:146–80. [PubMed: 18483144]

Mruk DD, Siu MKY, Conway AM, Lee NPY, Lau ASN, Cheng CY. Role of tissue inhibitor of metalloproteases-1 in junction dynamics in the testis. J Androl 2003;24:510–23. [PubMed: 12826691]

Mruk DD, Wong CH, Silvestrini B, Cheng CY. A male contraceptive targeting germ cell adhesion. Nat Med 2006;12:1323–8. [PubMed: 17072312]

Ono N, van der Heijden I, Scheffer GL, van de Wetering K, van Deemter E, de Haas M, Boerke A, Gadella BM, de Rooij DG, Neefjes JJ, Groothuis TAM, Oomen L, Brocks L, Ishikawa T, Borst P. Multidrug resistance-associated protein 9 (ABCC12) is present in mouse and boar sperm. Biochem J 2007;406:31–40. [PubMed: 17472575]

Robey RW, To KK, Polgar O, Dohse M, Fetsch P, Dean M, Bates SE. ABCG2: a perspective. Adv Drug Deliv Rev 2009;61:3–13. [PubMed: 19135109]

Sarkar O, Mathur PP, Cheng CY, Mruk DD. Interleukin-1 (IL1A) is a novel regulator of the blood-testis barrier in the rat. Biol Reprod 2008;78:445–54. [PubMed: 18057314]

Sarkar O, Xia W, Mruk DD. Adjudin-mediated junction restructuring in the seminiferous epithelium leads to displacement of soluble guanylate cyclase from adherens junctions. J Cell Physiol 2006;208:175–87. [PubMed: 16547975]

Schinkel AH, Smit JJM, van Tellingen O. Disruption of the mouse mdr1a P-glycoprotein gene leads to a deficiency in the blood-brain barrier and to increased sensitivity to drugs. Cell 1994;77:491–502. [PubMed: 7910522]

Seeger MA, van Veen HW. Molecular basis of multidrug transport by ABC transporters. Biochem Biophys Acta. 2008

Suzuki T, Onogawa T, Asano N, Mizutamari H, Mikkaichi T, Tanemoto M, Abe MA, Satoh F, Unno M, Shimosegawa T, Matsuno S, Ito S, Abe T. Identification and characterization of novel rat and human gonad-specific organic anion transporters. Mol Endocrinol 2003;17:1203–15. [PubMed: 12677006]

Thiebaut F, Tsuruo T, Hamada H, Gottesman MM, Pastan I, Willingham MC. Cellular localization of the multidrug-resistance gene product P-glycoprotein in normal human tissues. Proc Natl Acad Sci USA 1987;84:7735–8. [PubMed: 2444983]

Tsuruno T, Iida H. Effects of cytochalasins and colchicine on the accumulation and retention of daunomycin and vincristine in drug resistant tumor cells. Biochem Pharmacol 1986;35:1087–90. [PubMed: 3457567]

van Meer G, Halter D, Sprong H, Somerharju P, Egmond MR. ABC lipid transporters: extruders, flippases or flopless activators? FEBS Lett 2006;580:1171–7. [PubMed: 16376334]

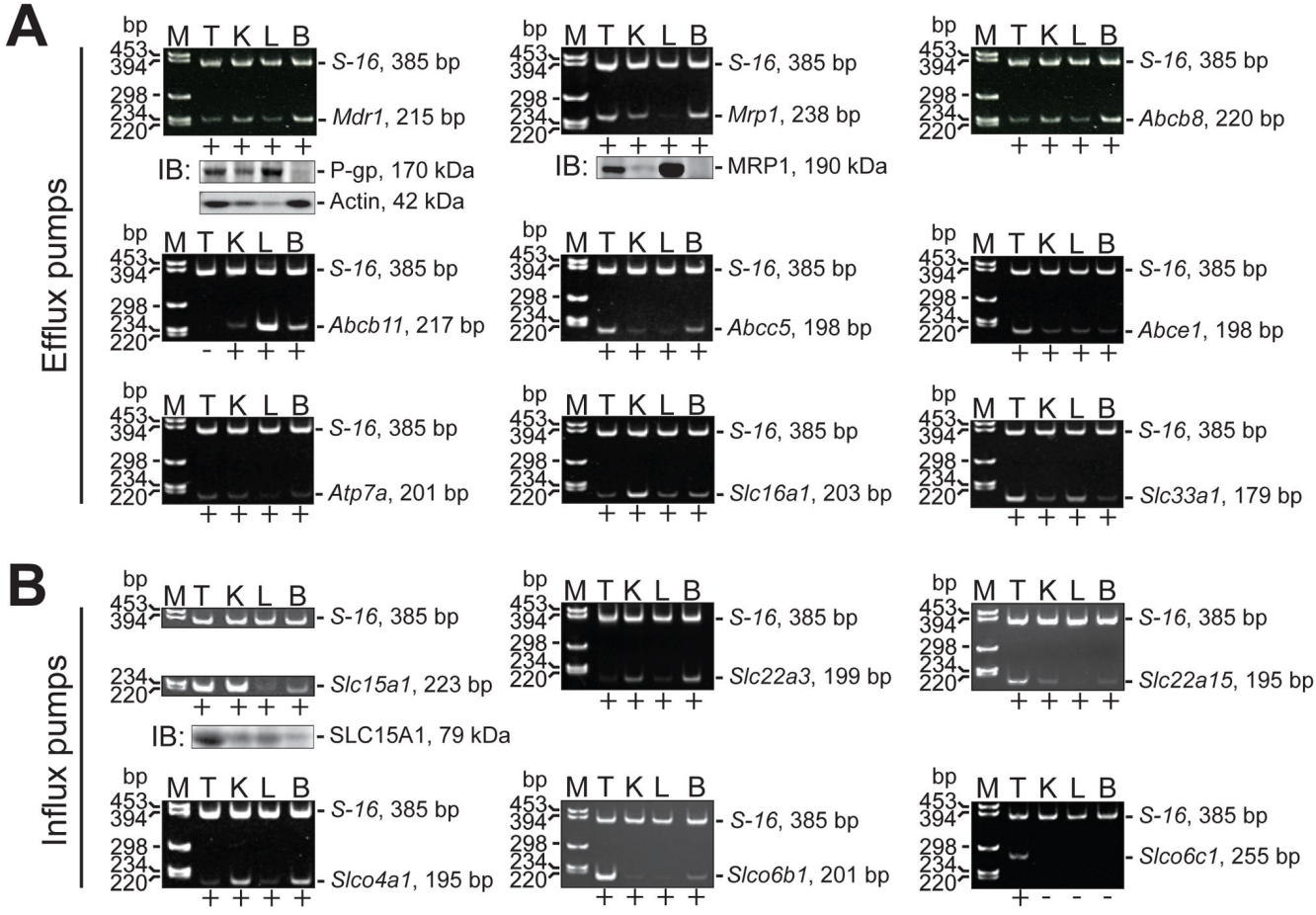

Figure 1. Efflux and influx pumps in different adult rat organs

A survey of efflux (**A**) and influx (**B**) pumps in testis (T), kidney (K), liver (L) and brain (B) was performed by RT-PCR and immunoblotting. The presence of an mRNA transcript within a specific tissue was noted by a "+" underneath each DNA gel image, whereas lack of an mRNA transcript was noted by a "–". The authenticity of mRNA transcripts detected in the testis was confirmed by nucleotide sequencing. S-16 (385 bp) and actin (42 kDa) were used as internal controls during RT-PCR and immunoblotting experiments, respectively. Amplicon sizes for each target gene are noted to the right of each gel image and in Table 1. Lanes in all immunoblots shown correspond to the same tissues used for RT-PCR experiments (*i.e.*, lane 1, T; lane 2, K; lane 3, L and lane 4, B). Details on primer design and antibodies are presented in Tables 1 and 2, respectively. M, marker; bp, base pairs; IB, immunoblotting.

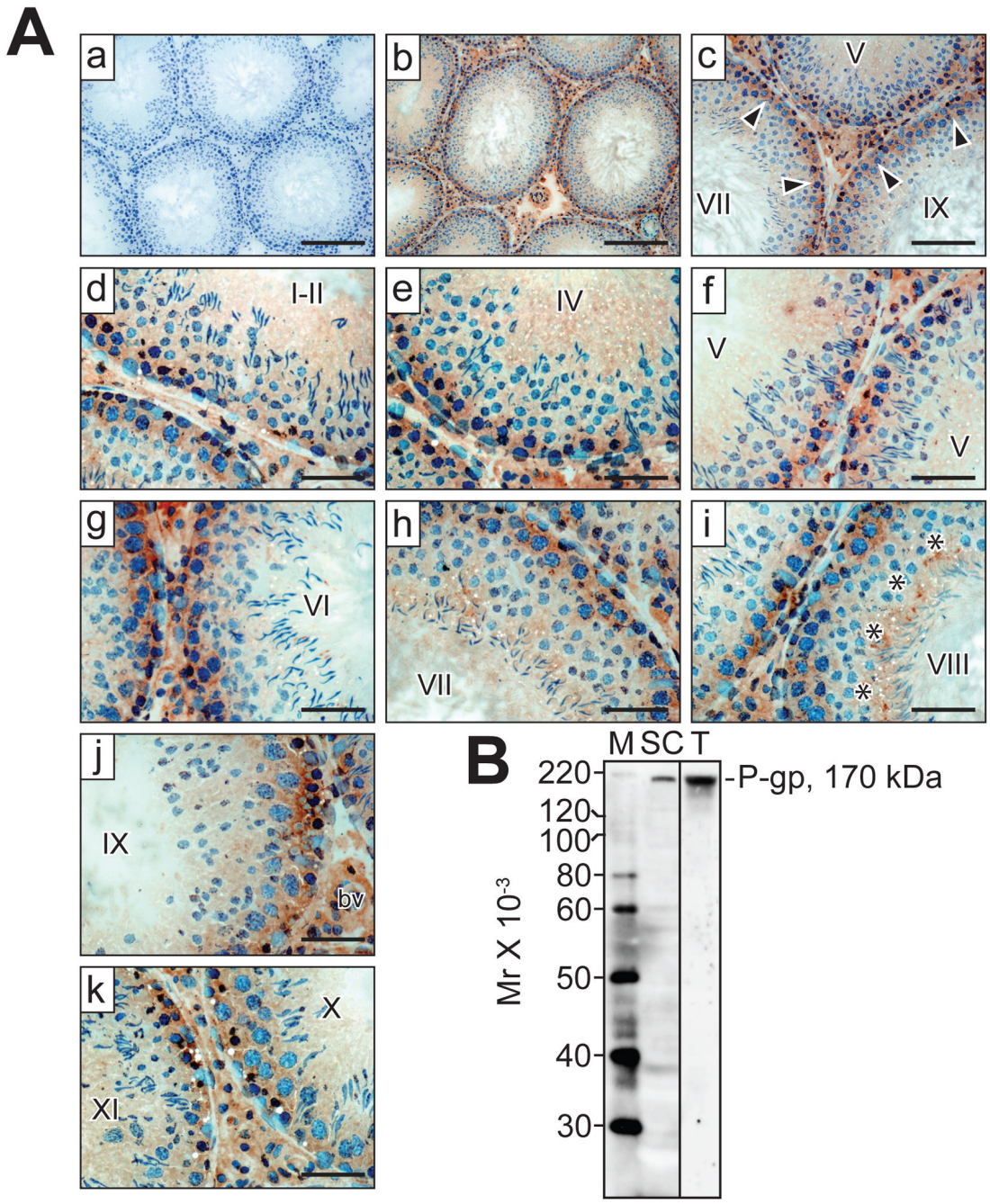

Figure 2. Localization of P-gp in the adult rat testis

(**A**) Immunohistochemistry was performed as described in *Materials and Methods* and Table 2. (**a–k**) Cross-sections of testis incubated with mouse (**a**, negative control) or P-gp (**b–k**) IgG. Arrowheads (**c**) point to the presence of immunoreactive P-gp (brownish precipitate) at the BTB at different stages of the seminiferous epithelial cycle (designated by roman numerals, **c–k**), whereas asterisks (**i**) point to the presence of P-gp at the apical ES at stage VIII. Nuclei were stained with hematoxylin. bv, blood vessel. Bars (**a**, **b**) = 160 μm; (**c**) = 100 μm; (**d–k**) = 50 μm. (**B**) Monospecificity of the P-gp antibody (Table 2; Santa Cruz Biotechnology, catalog #sc-55510, lot #B1108) when Sertoli cell (SC) and testis (T) lysates were used for SDS-PAGE and immunoblotting. A single protein of 170 kDa was observed. M, marker.

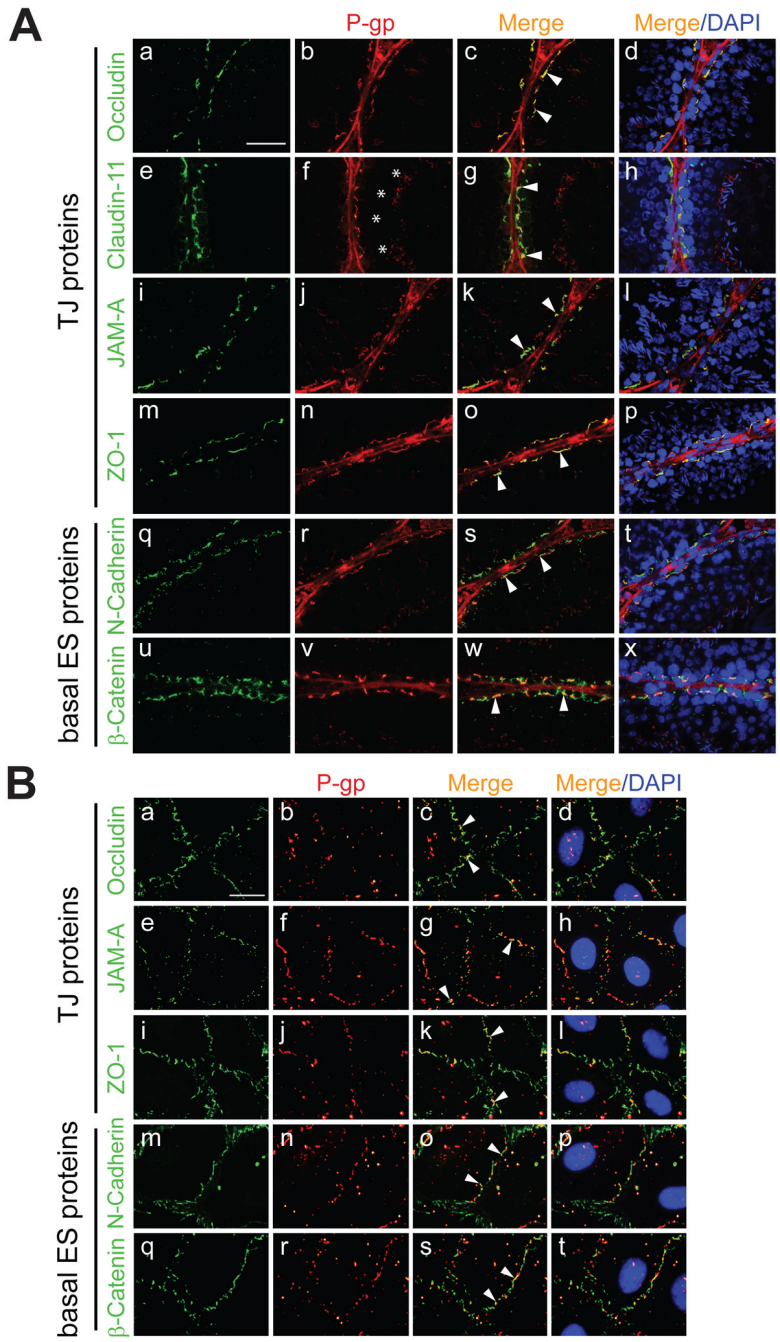

Figure 3. Co-localization of P-gp with constituent proteins of the BTB/Sertoli cell barrier *in vivo* and *in vitro*

Immunofluorescent microscopy was performed as detailed in *Materials and Methods* and Table 2. (**A**) Co-localization of either occludin (**a**, green), claudin-11 (**e**), JAM-A (**i**), ZO-1 (**m**), N-cadherin (**q**) or β-catenin (**u**) with P-gp (**b**, **f**, **j**, **n**, **r** and **v**, red) in the adult rat testis, respectively. Corresponding merged images (red + green and red + green + blue [DAPI]) are shown in (**c**, **d**, **g**, **h**, **k**, **l**, **o**, **p**, **s**, **t**, **w** and **x**). Arrowheads (**c**, **g**, **k**, **o**, **s** and **w**) point to areas of co-localization (orange-yellow). Asterisks (**f**) point to the presence of P-gp at the apical ES. Bar (**A**, **a**, also corresponds to **b–x**) = 50 μm. (**B**) Co-localization of either occludin (**a**, green), JAM-A (**e**), ZO-1 (**i**), N-cadherin (**m**) or β-catenin (**q**) with P-gp (**b**, **f**, **j**, **n** and **r**, red) in Sertoli cells (~0.05

$\times 10^6$ cells/cm^2) having a functional barrier 4 days after plating on Matrigel™-coated coverslips. Corresponding merged images are shown in (**c**, **d**, **g**, **h**, **k**, **l**, **o**, **p**, **s** and **t**). Arrowheads (**c**, **g**, **k**, **o** and **s**) point to areas of co-localization. Bar (**B**, **a**; also corresponds to **b–t**) = 23 μm. *In vivo* and *in vitro* experiments were repeated 3 times using different testes or batches of isolated Sertoli cells, respectively.

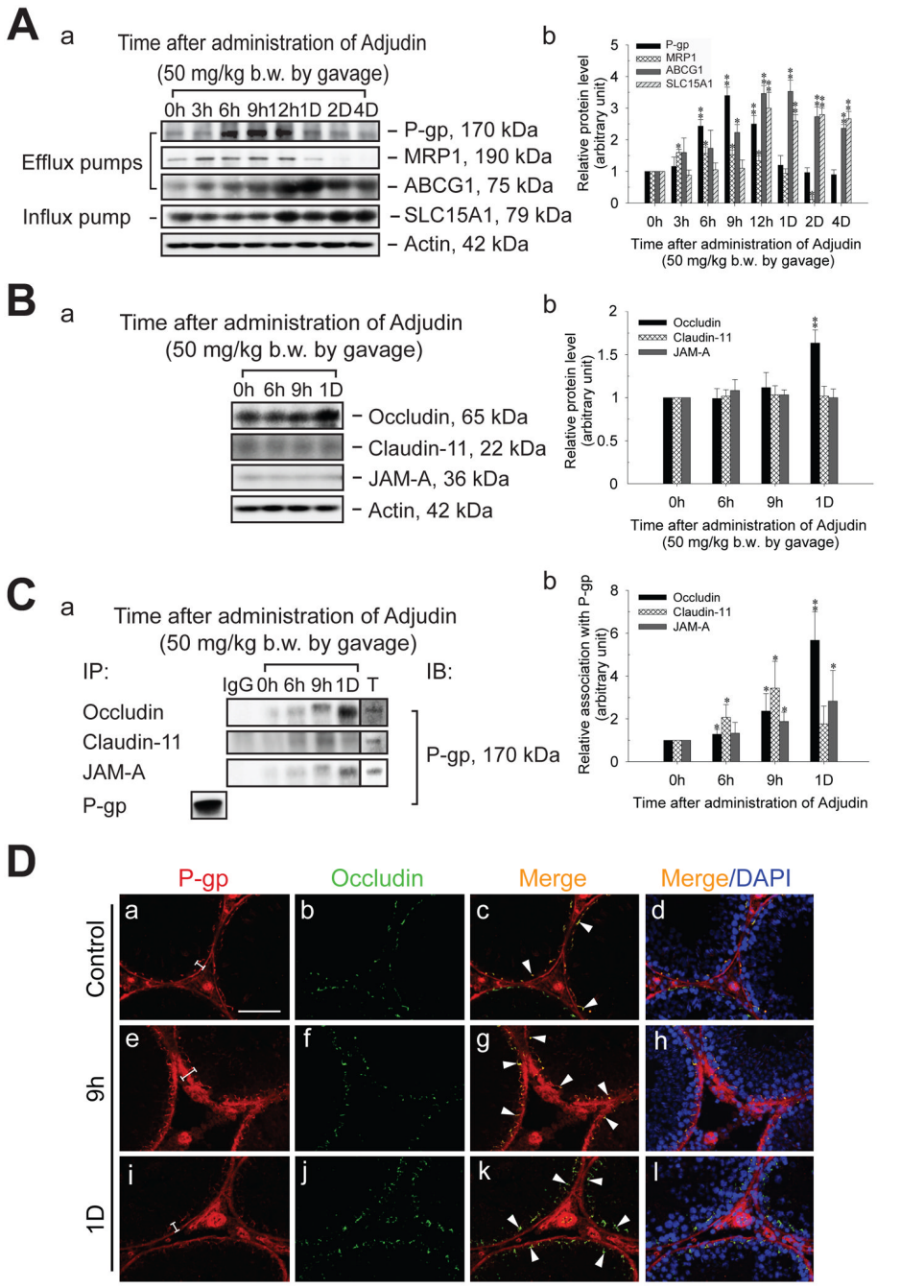

Figure 4. Changes in the steady-state levels of efflux/influx pumps, TJ proteins and protein-protein interactions in the testis following oral administration of Adjudin (50 mg/kg b.w.) to adult rats

(**A**, **a**) Immunoblots showing changes in P-gp, MRP1, ABCG1 and SLC15A1 in the testis after Adjudin treatment. Immunoblotting was performed as described in *Materials and Methods* and Table 2. (**A**, **b**) Histogram summarizing results shown in (**A**, **a**). (**B**, **a**) Immunoblots investigating the levels of occludin, claudin-11 and JAM-A in the testis after Adjudin treatment. (**B**, **b**) Histogram summarizing results shown in (**B**, **a**). Actin (**A**, **a** and **B**, **a**) was used to ensure equal sample processing. (**C**, **a**) Immunoblots corresponding to co-immunoprecipitation experiments using testis lysates from control (0 hr) and Adjudin-treated rats (6 and 9 hr [h], and 1 day [D]). The bottom row labeled as “P-gp” represents the use of adult testis lysate

(control, 500 μg) for co-immunoprecipitation (IP) and immunoblotting (IB); in this case, P-gp IgG (Table 2) was used for both IP and IB (positive control). The first lane labeled as "IgG" represents the use rabbit IgG instead of occludin, claudin-11 or JAM-A IgG for co-immunoprecipitation (negative control). The last lane labeled as "T" represents adult testis lysate (100 μg) without co-immunoprecipitation. Antibodies that were used for co-immunoprecipitation are listed under "IP" and in Table 2. (**C**, **b**) Histogram summarizing results of co-immunoprecipitation results shown in (**C**, **a**). Each bar in (**A**, **b; B**, **b** and **C**, **b**) represents mean ±SD of data from 4–7 separate experiments using testis lysate from different animals. *, $p<0.05$; **, $p<0.01$ (one-way ANOVA followed by Dunnett's test). (**D**) Co-localization of P-gp (**a**, **e** and **i**, red) with occludin (**b**, **f** and **j**, green) in control (**a–d**) and Adjudin-treated rat testes (**e–l**). Corresponding merged images are shown in (**c**, **d**, **g**, **h**, **k**, and **l**). Brackets (**a**, **e** and **i**) show an increase in P-gp staining. Arrowheads (**c**, **g** and **k**) point to areas of co-localization. Bar (**D**, **a**, also corresponds to **b–l**) = 100 μm.

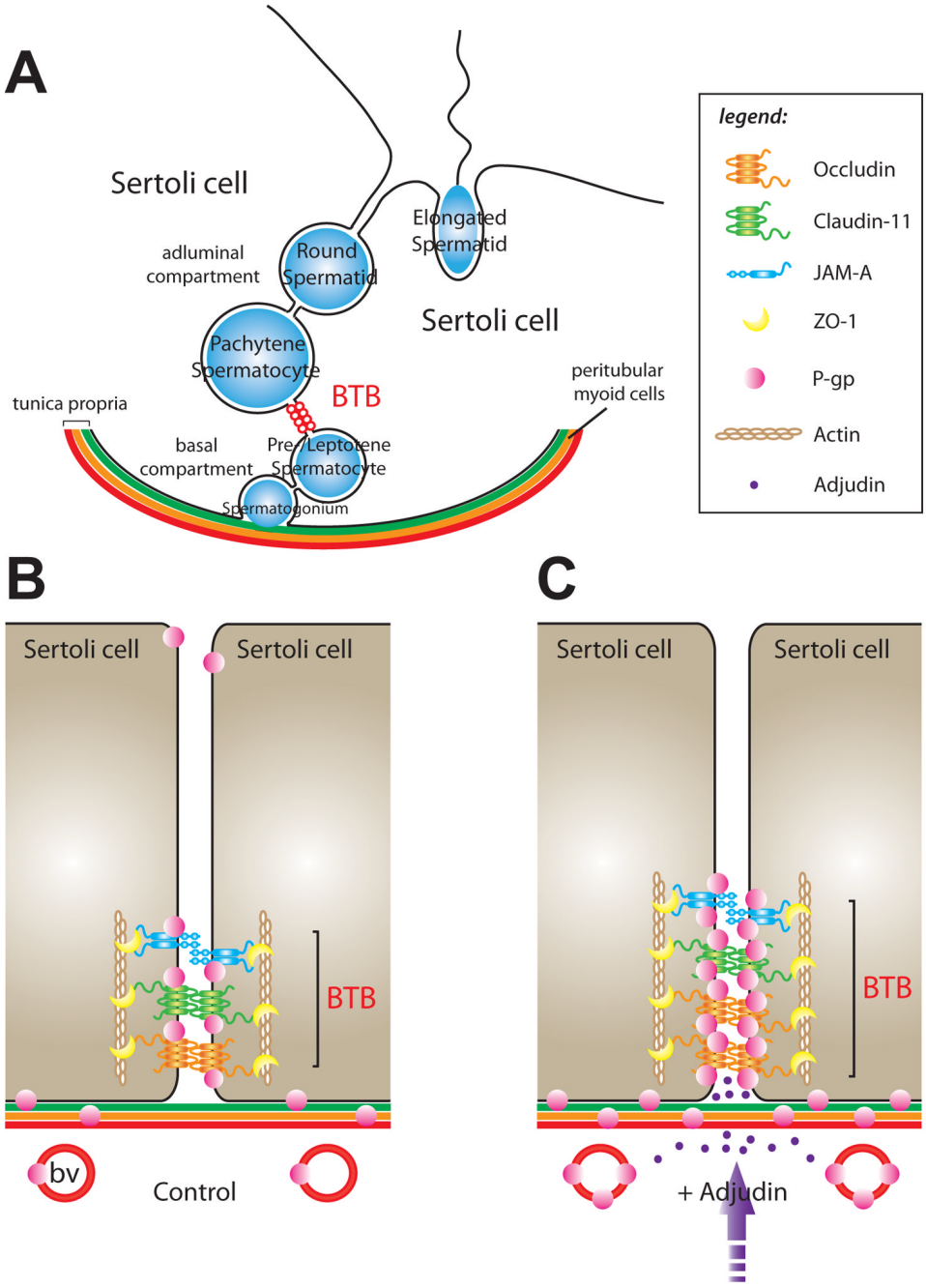

Figure 5. Model of P-gp function at the BTB

(**A**) Cross-section of the seminiferous epithelium in the adult rat testis. Pictured are two Sertoli cells situated atop the tunica propria which is composed of: (i) the basement membrane, (ii) a layer of type I collagen, (iii) peritubular myoid cells (depicted as the orange layer), (iv) lymph and (v) the lymphatic endothelium. The BTB (depicted as red-colored open circles) physically divides the seminiferous epithelium into basal and adluminal compartments. Also shown are different types of differentiating germ cells (depicted as blue-colored circles/oval). (**B**) A magnified view depicting some of the molecular components of the BTB in the adult rat testis (control). The key TJ proteins that are represented in this panel are those that were included in co-immunoprecipitation experiments (Figure 4); basal ES proteins such as N-cadherin and β-

catenin, which are also present at the BTB, are not shown. P-gp localized to the BTB, the Sertoli cell-elongated spermatid interface, peritubular myoid cells and blood vessel (bv) endothelia. (**C**) A magnified view depicting changes in protein-protein interactions at the BTB following oral administration of Adjudin (+ Adjudin). During assault of the seminiferous epithelium by Adjudin (*i.e.*, Sertoli-germ cell junction restructuring), P-gp associated more with occludin, claudin-11 and JAM-A (Figure 4), possibly to enhance BTB function. A 'tighter' barrier may block further entry of Adjudin into the seminiferous epithelium. Following Adjudin treatment, more P-gp was also found to associate with peritubular myoid cells (note: in rodents, these cells are known to contribute to BTB integrity) and blood vessel endothelia. For simplicity, germ cells were not included in (**B**) and (**C**). The legend corresponds to panels (**B**) and (**C**).

Table 1

Primers used for RT-PCR experiments in this study.

Function	Gene	Primer sequence	Orientation	Position	Length (bp)	Annealing Temp. (°C)	Cycle No.	GenBank® Accession No.
Efflux pumps	*Mdr1a*[1]	5′-ATGACACCCCTGAAATCCA-3′ 5′-CGCTCCTGTGGTGTTTTTA-3′	sense anti-sense	2201–2219 2397–2415	215	54	28	AF257746
	Mrp1	5′-CCTACTACCCCAGCATTGT-3′ 5′-TATTCCTTCAGTCTCTCCAC-3′	sense anti-sense	3566–3584 3784–3803	238	54	24	AY170916
	Abcb8	5′-TTTCGTGTCTGAGTCCCGTA-3′ 5′-CACATCAGTAGTCAAGCGG-3′	sense anti-sense	504–523 705–723	220	52	27	DQ233644
	Abcb11	5′-TCTACGCAGGAGTCGGCAT-3′ 5′-TGGTCGGCAATGGCGTCA-3′	sense anti-sense	431–449 630–647	217	53	35	NM_031760
	Abcc5	5′-GGCAGAGGATGTTTGAAGC-3′ 5′-CGGCTACACACTTTCTCCT-3′	sense anti-sense	851–869 1030–1048	198	53	27	NM_053924
	Abce1	5′-AAAAGTTGCCCCGTAGTCC-3′ 5′-GCGATGTGTTGTTTCTTTTTCC-3′	sense anti-sense	79–97 237–258	180	53	25	NM_001108446
	Atp7a	5′-TGCTGAAGATGAGAGTGGAA-3′ 5′-TTATGAAGGCTGGAAAACCC-3′	sense anti-sense	515–534 696–715	201	52	32	NM_052803
	Slc16a13	5′-TTACTTCTCTCAGCGACGAT-3′ 5′-CAGTGTCTTCAGTCAGGG-3′	sense anti-sense	393–412 578–595	203	53	27	NM_001005530
	Slc33a1	5′-CAGAGAAGCGTCAGTAGTAAA-3′ 5′-GCACTCCCTCTTCTACCA-3	sense anti-sense	846–866 1007–1024	179	53	25	BC078832
Influx pumps	*Slc15a1*	5′-CTCTGCTACCTGACTCCAA-3′ 5′-TACCAAGGGCTATCAGGG-3′	sense anti-sense	184–202 389–406	223	53	35	NM_057121
	Slc22a3	5′-CACCTTCGCCTTCCTCTTC-3′ 5′-TTCCAGCAGGTAGCGGTGA-3′	sense anti-sense	90–108 270–288	199	55	37	NM_019230
	Slc22a15	5′-CTCACAGGTTTTGCTCTTG-3′ 5′-AAAGAAGAGACCGCCAATC-3′	sense anti-sense	427–445 603–621	195	52	29	NM_001107707
	Slco4a1	5′-TGTTTGAGCCCCAGGTTGA-3′ 5′-AGCCGTTCACTGTCATACC-3′	sense anti-sense	170–188 346–364	195	53	28	NM_133608
	Slco6b1	5′-CATCAGAGTATTCCCTTATCA-3′ 5′-CAGAACGAGATAAGAAAGAAG-3′	sense anti-sense	249–269 429–449	201	52	27	NM_133412
	Slco6c1	5′-TTTCTTCATCATTGGGCAGTGT-3′ 5′-TTCCACCACCCAAACTGC-3′	sense anti-sense	642–663 879–896	255	54	25	NM_173338

[1]In rodents, *Mdr1* is encoded by two genes, *Mdr1a* and *Mdr1b*, which share an overall nucleotide homology of ~88%. Sense and anti-sense primers were designed to anneal to two short stretches of sequence corresponding to *Mdr1a* (listed above) which shared ~75% and ~84% homology with *Mdr1b*, respectively. Although nucleotide sequencing revealed the mRNA transcript in the testis to be *Mdr1a* (Figure 1A) and *Mdr1a* (but not *Mdr1b*) is expressed predominantly in the testis, there is the remote possibility that we amplified *Mdr1b* instead of *Mdr1a*. As such, we have cautiously labeled this PCR product as *Mdr1* in Figure 1A.

Table 2

Summary of primary antibodies used in this study.

Antigen	Catalog #	Lot #	Immunogen	Host	Vendor	Working dilution			
						IB	IHC	IF	IP
P-gp	sc-55510	B1108	Amino acid residues 1040–1240 of human MDR1	Mouse	Santa Cruz Biotechnology	1:200	1:50	1:50	
	ab3364[1]	418401	SDS-solubilized plasma membranes from multidrug resistant cell lines	Mouse	Abcam	1:500			
	517310[1]	D00022523	SDS-solubilized plasma membranes from multidrug resistant cell lines	Mouse	Calbiochem	1:250			
MRP1	sc-13960	I1906	Amino acid residues 1–70 of human MRP1	Rabbit	Santa Cruz Biotechnology	1:200			
ABCG1	ab52617	467040	Synthetic peptide corresponding to human ABCG1	Rabbit	Abcam	1:2000			
SLC15A1	LS-C188551	2477	Synthetic peptide corresponding to human SLC15A1	Rabbit	Lifespan biosciences	1:1000			
Occludin	71–1500	00250207	Fusion protein corresponding to C-terminus of human occludin	Rabbit	Zymed/Invitrogen	1:400		1:50	1:40
JAM-A	36–1700	370923A	Synthetic peptide derived from the C-terminus of human JAM-A	Rabbit	Zymed/Invitrogen	1:250		1:50	1:40
Claudin-11	36–4500	387613A	Synthetic peptide derived from the C-terminus of human claudin-11	Rabbit	Zymed/Invitrogen	1:125		1:50	1:40
ZO-1	61–7300	389452A	Fusion protein corresponding to amino acid residues 463–1109 of human ZO-1	Rabbit	Zymed/Invitrogen	1:250		1:50	
N-Cadherin	sc-7939	H0907	Amino acid residues 450–512 of human N-cadherin	Rabbit	Santa Cruz Biotechnology			1:50	
β-Catenin	71–2700	60806848C2	Synthetic peptide derived from the C-terminus of human/mouse/rat β-catenin	Rabbit	Zymed/Invitrogen			1:50	
Actin	sc-1616	F2007	Peptide mapping of C-terminus of human actin	Goat	Santa Cruz Biotechnology	1:200			

IB, immunoblotting; IHC, immunohistochemistry; IF, immunofluorescence; IP, immunoprecipitation.

[1]These antibodies were only used to verify immunoblotting results.